J. Membrane Biol. 134, 131–142 (1993)

The Journal of
Membrane
Biology
© Springer-Verlag New York Inc. 1993

# ATP-Inhibited and $Ca^{2+}$-Dependent $K^+$ Channels in the Soma Membrane of Cultured Leech Retzius Neurons

**Gudrun Frey, Wolfgang Hanke, Wolf-R. Schlue**

Institut für Zoologie/Lehrstuhl für Neurobiologie, Heinrich-Heine-Universität Düsseldorf, Universitätsstr. 1, D-4000 Düsseldorf, FRG

Received: 24 September 1992/Revised: 25 January 1993

**Abstract.** The properties of one ATP-inhibited and one $Ca^{2+}$-dependent $K^+$ channel were investigated by the patch-clamp technique in the soma membrane of leech Retzius neurons in primary culture. Both channels rectify at negative potentials. The ATP-inhibited $K^+$ channel with a mean conductance of 112 pS is reversibly blocked by ATP ($K_i$ = 100 $\mu$M), TEA ($K_i$ = 0.8 mM) and 10 mM $Ba^{2+}$ and irreversibly blocked by 10 nM glibenclamide and 10 $\mu$M tolbutamide. It is $Ca^{2+}$ and voltage independent. Its open state probability ($P_o$) decreases significantly when the pH at the cytoplasmic face of inside-out patches is altered from physiological to acid pH values. The $Ca^{2+}$-dependent $K^+$ channel with a mean conductance of 114 pS shows a bell-shaped $Ca^{2+}$ dependence of $P_o$ with a maximum at pCa 7–8 at the cytoplasmic face of the membrane. The $P_o$ is voltage independent at the physiologically relevant $V$ range. $Ba^{2+}$ (10 mM) reduces the single channel amplitude by around 25% (ATP, TEA, glibenclamide, tolbutamide, and $Ba^{2+}$ were applied to the cytoplasmic face of the membrane).

We conclude that the ATP-dependent $K^+$ channel may play a role in maintaining the membrane potential constant—independently from the energy state of the cell. The $Ca^{2+}$-dependent $K^+$ channel may play a role in generating the resting membrane potential of leech Retzius neurons as it shows maximum activity at the physiological intracellular $Ca^{2+}$ concentration.

**Key words:** Leech — Potassium channel — Patch clamp — ATP — pH — Sulfonylureas

## Introduction

Various types of $K^+$ channels with distinctive biophysical properties have been identified and characterized in excitable and nonexcitable cells. These channels differ with respect to their pharmacological specificities, kinetics and ion selectivity (*for review see*, e.g., Latorre & Miller, 1983; Schwarz & Passow, 1983; Ashcroft, 1988; Rudy, 1988; Ashcroft & Ashcroft, 1990; Kolb, 1990). In nervous systems, $K^+$ channels are involved in generating the resting membrane potential and they play an important role in regulating the level of neuronal excitability, information coding and integration. The requirement for a large repertoire of neuronal firing patterns may therefore underlie the need for a diversity of $K^+$ channels (*cf.* Rudy, 1988).

In the membrane of leech neurons different types of voltage-dependent $K^+$ channels have been characterized on the macroscopical level, but very little is known about the properties of $K^+$ channels on the single channel level. In growth cones of leech Retzius neurons three $K^+$ currents were detected (Garcia et al., 1990): A rapidly activating and inactivating A-type $K^+$ current, a more slowly activating and inactivating delayed $K^+$ current, and a $Ca^{2+}$-activated $K^+$ current. In the axonal stump of Retzius neurons Bookman and Dagan (1987) have already described a 35 pS and a 20 pS $K^+$ channel.

The present study was undertaken to investigate $K^+$-selective ion channels in the soma membrane of leech Retzius neurons in more detail. Retzius neurons have the largest cell bodies within the leech central nervous system and are easily identifiable. They can be isolated from single ganglia and maintained in tissue culture for up to two weeks (Dietzel,

Drapeau & Nicholls, 1986). Some functional roles of these neurons in the integrative behavior of the leech have been suggested, e.g., the control of mucus secretion from the skin (Lent, 1973), the effects on the tension of body wall muscle (Mason & Kristan, 1982), and a probable role in the regulation of swimming (Willard, 1981).

We recorded single channel activity in the cell-attached and inside-out configuration (Hamill et al., 1981). We characterized two types of $K^+$ channels: one type is sensitive to internal adenosine-5′-triphosphate (ATP) and the other type is dependent on the intracellular $Ca^{2+}$ concentration.

## Materials and Methods

Retzius neurons from the central nervous system of the medicinal leech, *Hirudo medicinalis*, were isolated from single ganglia as follows (for leech preparation *see* Schlue & Deitmer, 1980): After opening the ganglion capsule with a miniature needle, the ganglia were enzyme treated with collagenase/dispase (Boehringer-Mannheim; 0.5 mg/ml in modified Leibovitz-15 medium) for three hours. Retzius neurons which were identified by their size and position in the ganglion were then removed by means of a fire-polished suction pipette (diameter 100–150 $\mu$m) (Dietzel et al., 1986). The Retzius neurons were kept in culture dishes (Nunc) in modified Leibovitz-15 medium at 20°C for up to two weeks. The modified Leibovitz-15 medium (abbreviated as L-15) contained: 100 ml Leibovitz-15 medium with glutamine (cations in mM: 144.7 $Na^+$, 5.8 $K^+$, 1.4 $Ca^{2+}$, 1.8 $Mg^{2+}$; GIBCO), 25 mM $\alpha$-D-glucose, 1 ml gentamicin (GIBCO), 2 ml heat-inactivated fetal calf serum (GIBCO), 10 mM HEPES (N-2 hydroxyethylpiperazine-N′-2-ethanesulfonic acid, Roth) adjusted to pH 7.4 with NaOH.

Patch-clamp recordings were performed on the soma membrane of Retzius neurons according to the method of Neher and Sakmann (*cf.* Hamill et al., 1981). Ionic currents from single potassium channels were recorded in the cell-attached and inside-out configuration. All experiments were carried out at room temperature (20–25°C). During experiments in the inside-out configuration the bathing solution was exchanged by means of a single-barreled perfusion pipette (up to 12 solutions could be handled by a valve; the exchanging time was less than 15 sec).

The standard bathing solution (120 mM $K^+$ solution) and the pipette solution contained in mM: 120 KCl, 1 $CaCl_2$, 10 HEPES adjusted to pH 7.4 with KOH. In ion selectivity measurements KCl was replaced by $NH_4Cl$ and RbCl in equimolar amounts. Solutions with $Ca^{2+}$ levels below 1 mM were prepared according to Ammann et al. (1987) [120 mM $K^+$ solution pCa X]. The solutions with altered pH values contained 120 mM KCl, 1 mM $CaCl_2$ and 10 mM buffer (*see* 120 mM $K^+$ solution) [10 mM PIPES (piperazine-N,N′-bis[2-ethane-sulfonic acid], Sigma) for pH 6.1 and 6.5, 10 mM HEPES for pH 7.0 and 7.5 or 10 mM TAPS (N-tris[Hydroxymethyl]methyl-3-amino-propanesulfonic acid, Sigma) for pH 8.0, 8.5 and 9.0; 120 mM $K^+$ solution pH X]. TEA (tetraethylammoniumchloride, Merck-Schuchardt), $Cs^+$, $Ba^{2+}$, ATP (adenosine 5′-triphosphate dipotassium salt, vanadium-free; Sigma), and ATP-$\gamma$-S (adenosine 5′-O-[3-thiotriphosphate], Sigma) were added to the 120 mM $K^+$ solution shortly before use. These ATP-containing solutions were nominally $Mg^{2+}$-free. Stock solutions of tolbutamide and glibenclamide were prepared in 0.1 M KOH (20 mM) and added to the 120 mM $K^+$ solution to provide the desired final concentrations.

Patch pipettes were pulled from borosilicate glass capillaries (outer diameter 1.5 mm, Clark GC150F-10) using a two-stage horizontal microelectrode puller (Mecanex SA BB-CH) (pipette resistance 30–50 M$\Omega$). A standard patch-clamp setup as described by Hamill et al. (1981) was used. The signal was amplified by an L/M-EPC7 List amplifier and filtered at 2 kHz by an 8-pole low-pass filter (Rockland). Data were digitized at a 4 kHz rate by a Labmaster TL-1 interface, recorded and analyzed on a computer using the pCLAMP 5.5 program (Axon Instruments). Amplitude histograms and idealized traces for kinetic analysis were constructed from recordings stored on the hard disk of an IBM-compatible computer. The open state probabilities ($P_o$) were determined as follows: Integral amplitude histograms were constructed from the recordings. The peaks belonging to the open and closed states were defined and the area beneath each peak was integrated. The ratio of the area of each open state and of the total area was defined as $P_o$. $P_o$ was calculated on an IBM-compatible computer using a program written by the authors. Channel-state lifetimes were evaluated by fitting sums of exponentials in the lifetime distribution as obtained from the idealized traces. The single channel conductances were calculated from the linear portion of the corresponding $I/V$ plots with 120 mM $K^+$ solution on both sides of the membrane patch. The potentials are denoted according to the physiological definition. In all figures cation fluxes from pipette to bath are shown as upward deflections and negative in sign. The closed states are marked by bars.

## Results

Patch-clamp experiments were carried out on the soma membrane of leech Retzius neurons in primary culture. In the following we characterize the ATP, $Ca^{2+}$, pH and voltage dependence, the ion selectivity and pharmacology of one ATP-inhibited and one $Ca^{2+}$-dependent $K^+$ channel in the cell-attached and inside-out configuration. The mean channel conductance is 112 pS of the ATP-inhibited and 114 pS of the $Ca^{2+}$-dependent $K^+$ channel in symmetrical 120 mM $K^+$ solution. These $K^+$ channels did not "run down" when changing from the cell-attached to the cell-free configuration. Furthermore, they showed no inactivation in 30 min at our experimental conditions.

### ATP-Inhibited $K^+$ Channel

The properties of an ATP-inhibited $K^+$ channel are shown in Fig. 1: (*A*) shows recordings, (*B*) the amplitude histogram, (*C*) and (*E*) the lifetime distributions of the closed states and (*D*) and (*F*) the lifetime distributions of the open states (inside-out configuration, −40 mV holding potential, symmetrical 120 mM $K^+$ solution). We separated fast (*C, D*) and slow (*E, F*) kinetics of the bursting behavior. The mean state lifetimes are $t_{o,f}$ = 1.3 msec, $t_{c,f}$ = 0.2 msec, $t_{o,s}$ = 28.8 msec, $t_{c,s1}$ = 3.8 msec and $t_{c,s2}$ = 49.3 msec ($s$ = slow bursting kinetics; $f$ = fast kinetics

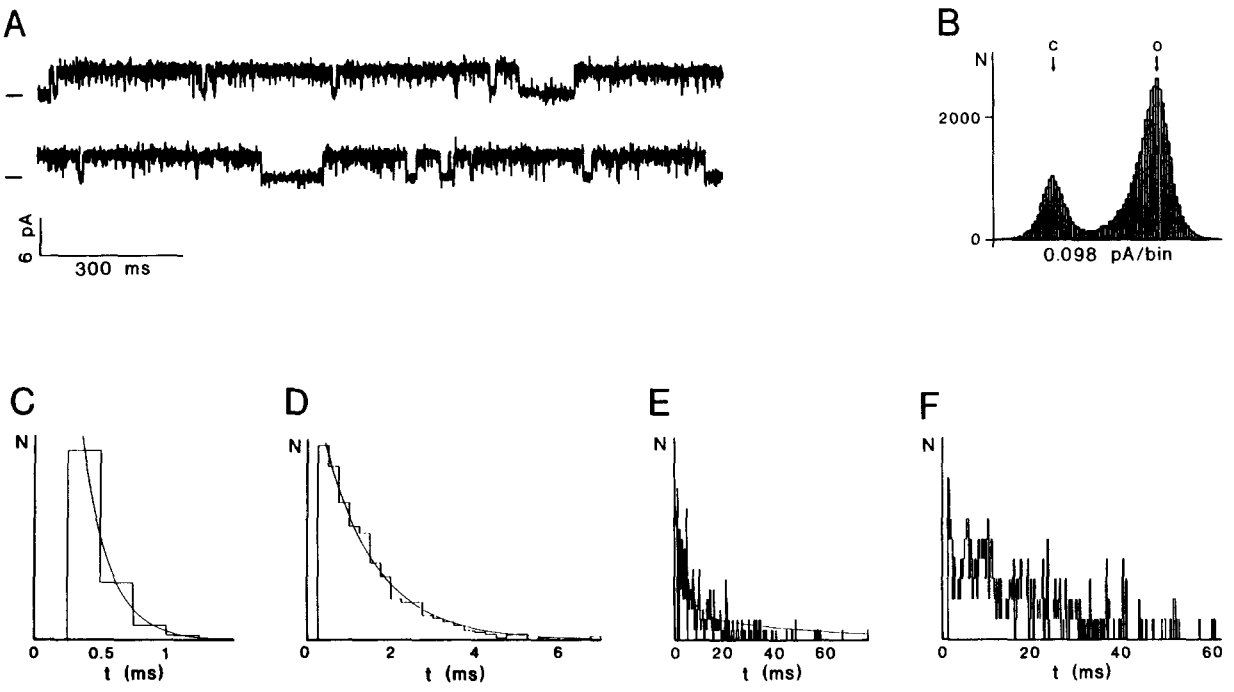


**Fig. 1.** Properties of an ATP-inhibited $K^+$ channel: Recordings (*A*), amplitude histogram (*B*), and lifetime distribution of the closed (*C, E*) and open (*D, F*) states [inside-out configuration, symmetrical 120 mM $K^+$ solution, −40 mV holding potential]. The slow bursting kinetics (*s*; *E, F*) and the fast kinetics within bursts (*f*; *C, D*) are separated. The different state lifetimes are $t_{c,s1}$ = 3.8 msec, $t_{c,s2}$ = 49.3 msec, $t_{o,s}$ = 28.8 msec, $t_{c,f}$ = 0.2 msec, and $t_{o,f}$ = 1.3 msec.

within bursts). The $P_o$ of this channel amounts to 0.83.

## ATP-Inhibition

$P_o$ of the ATP-inhibited $K^+$ channel increases during the first minute after changing from the cell-attached to the inside-out configuration (Fig. 2*A*: upper two recordings). The enhancement of $P_o$ is found in L-15 as well as in 120 mM $K^+$ solution as bathing medium. On adding 2 mM ATP to the cytoplasmic face of the excised patch $P_o$ decreases almost to the cell-attached value within 1 min (Fig. 2*A*: +ATP, lower recording). ATP reversibly reduces $P_o$ by increasing the closed and decreasing the open times, but it does not affect the single channel amplitude. $P_o$ in the presence of ATP standardized to $P_o$ in the absence of ATP ($P_o$, ATP/$P_o$) is plotted *vs.* the ATP concentration in the bathing solution in Fig. 2*B* ($n$ = 17). ATP (100 $\mu$M) is required for half-maximal inhibition of channel activity ($K_i$) at the cytoplasmic face of the membrane (inside-out configuration, symmetrical 120 mM $K^+$ solution, −40 mV holding potential). The blocking effect of ATP is most probably not due to a phosphorylation process since (i) 100 $\mu$M of the unhydrolyzable ATP-γ-S also blocks the ATP-inhibited $K^+$ channel by about 50% ($n$ = 3; Fig. 3) and (ii) the presence of $Mg^{2+}$ is not required for channel inhibition.

## Ion Selectivity, Rectification and Voltage Dependence

Ion substitution experiments at the cytoplasmic face of inside-out patches reveal that the ATP-inhibited $K^+$ channel is selective for $K^+$ over $Na^+$, $NH_4^+$, and $Rb^+$. Figure 4 shows the *I/V* plot of the channel with 120 mM $K^+$ solution and L-15 as bathing solution. The *I/V* plot with L-15 as bathing solution rectifies at positive potentials and reveals a reversal potential of about +60 mV. From this value and the salt concentrations given in Materials and Methods a permeability coefficient ($P_K/P_{Na}$) of 25 was calculated according to the Goldman-Hodgkin-Katz-equation.

The *I/V* plots in the cell-attached configuration (L-15 as bathing solution) and in the inside-out configuration (120 mM $K^+$ solution as bathing solution) show that the channel rectifies at negative voltages (outward rectification). The *I/V* plot in the inside-out configuration in symmetrical 120 mM $K^+$ solution

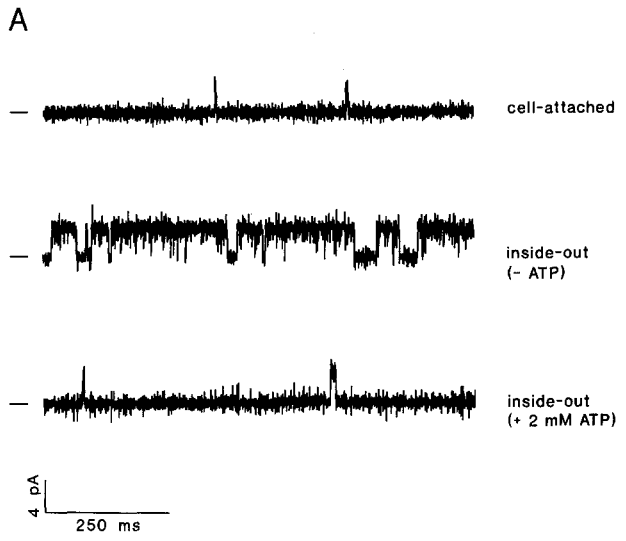


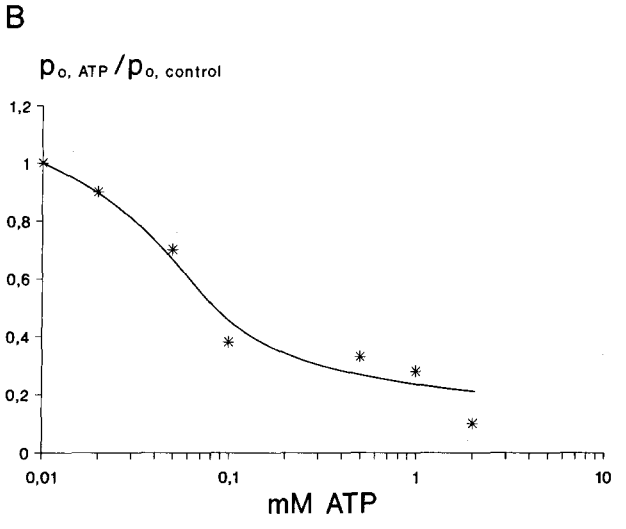


**Fig. 2.** ATP-sensitivity of the ATP-inhibited $K^+$ channel. Recordings in the cell-attached and in the inside-out configuration in the absence (−ATP) and presence (+ATP) of 2 mM ATP in the bathing solution (*A*); relation between ATP concentration in the bathing solution and $P_o$ standardized to $P_o$ in the absence of ATP (*B*) [inside-out configuration, symmetrical 120 mM $K^+$ solution, −40 mV holding potential]. $P_o$ of the ATP-inhibited $K^+$ channel in *A* increased during the first minute after excising the patch (upper two recordings), the addition of 2 mM ATP to the cytoplasmic face of the membrane reduced $P_o$ almost to the cell-attached value (lower recording). The $P_{o,\,ATP}/P_{o,\,control}$/[ATP]-plot in *B* reveals a $K_i$ value of 100 μM ATP.

reveals a saturation at positive voltages above +80 mV.

The *I/V* plot in the cell-attached configuration cuts the abscissa at about 50 mV. This indicates a membrane potential of about −50 mV under our culturing conditions which is in accordance to the measured membrane potential of −47.3 ± 5.5 mV (Schlue & Deitmer, 1988).

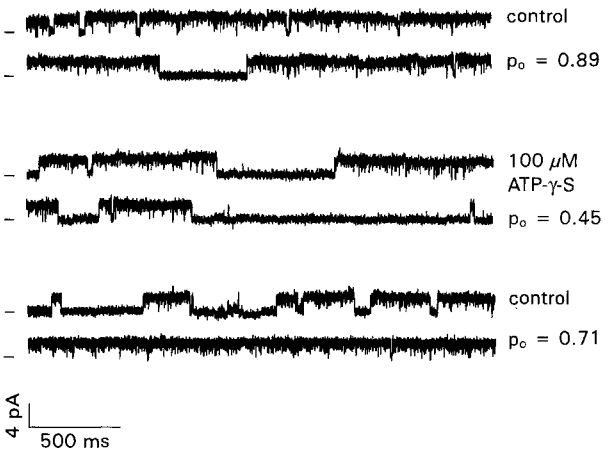


**Fig. 3.** ATP-γ-S sensitivity of the ATP-inhibited $K^+$ channel. Recordings in the inside-out configuration before ATP-γ-S application (control, upper recording), in the presence of 100 μM ATP-γ-S in the bathing solution and after removal of ATP-γ-S (control, lower recording) (symmetrical 120 mM $K^+$ solution, −40 mV holding potential). The addition of 100 μM ATP-γ-S to the cytoplasmic face of the membrane reduced $P_o$ of this channel by 50% from 0.89 to 0.45. After removing ATP-γ-S $P_o$ increased back to 0.71. The discrepancy between the two control values is probably due to an incomplete removal of ATP-γ-S.

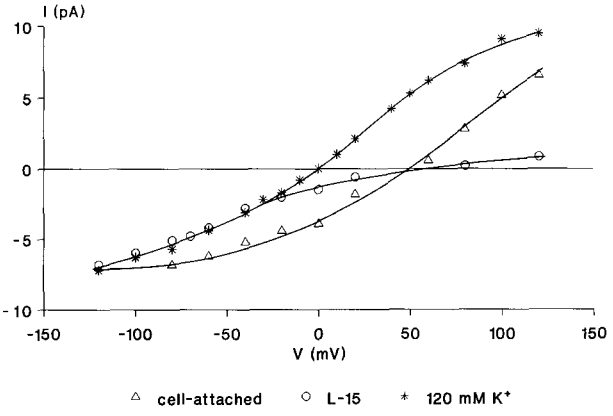


**Fig. 4.** Ion selectivity and rectification of the ATP-inhibited $K^+$ channel. The *I/V* plots in the inside-out configuration with 120 mM $K^+$ solution ($n$ = 12) and with L-15 as bathing solution ($n$ = 9) indicate that the ATP-inhibited $K^+$ channel is selective for $K^+$ over $Na^+$: The *I/V* plot with L-15 as bathing solution bends at positive voltages and reveals a reversal potential of about +60 mV. According to the Goldman-Hodgkin-Katz-equation a permeability coefficient ($P_K/P_{Na}$) of 25 can be calculated.

The *I/V* plots in the cell-attached (L-15 as bathing solution, $n$ = 5) and in the inside-out configuration in symmetrical 120 mM $K^+$ solution demonstrate the rectifying characteristics of this channel type at negative voltages. The *I/V* plot in the inside-out configuration in 120 mM $K^+$ solution shows a saturation at positive voltages above +80 mV. This saturation may occur at more positive voltages in the cell-attached configuration, but because of the instability of seals at high positive voltages data could not be obtained.

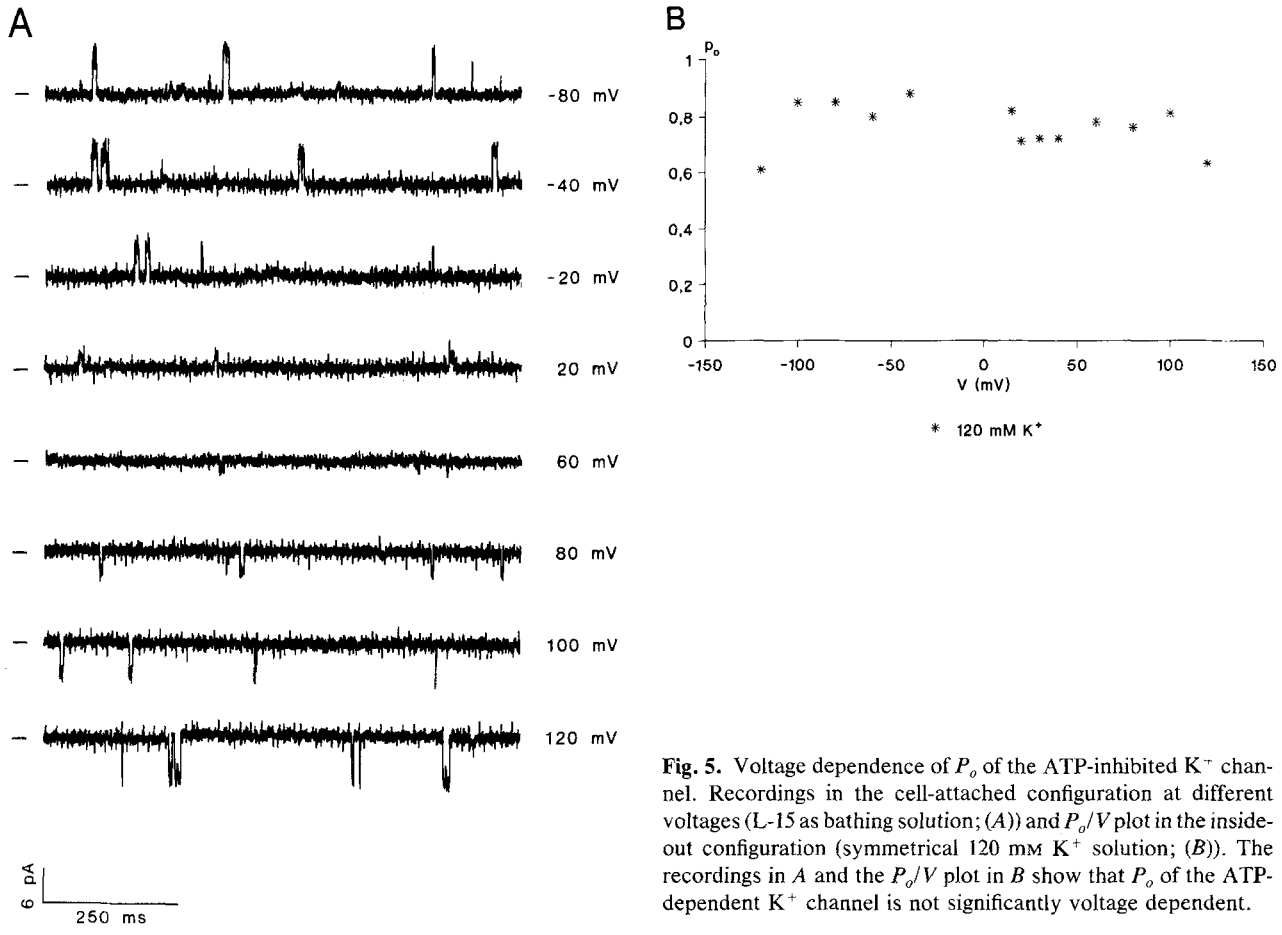


**Fig. 5.** Voltage dependence of $P_o$ of the ATP-inhibited $K^+$ channel. Recordings in the cell-attached configuration at different voltages (L-15 as bathing solution; (*A*)) and $P_o/V$ plot in the inside-out configuration (symmetrical 120 mM $K^+$ solution; (*B*)). The recordings in *A* and the $P_o/V$ plot in *B* show that $P_o$ of the ATP-dependent $K^+$ channel is not significantly voltage dependent.

The voltage dependence of the ATP-inhibited $K^+$ channel was analyzed in cell-attached and inside-out patches (Fig. 5). Figure 5*A* shows recordings of an ATP-inhibited $K^+$ channel in a cell-attached patch at different voltages (L-15 as bathing solution) and Fig. 5*B* a $P_o/V$ plot in the inside-out configuration (symmetrical 120 mM $K^+$ solution). $P_o$ of the ATP-inhibited $K^+$ channel does not show a significant voltage dependence either in the cell-attached or in the inside-out configuration. $P_o$ has values of about 0.01 ($n = 5$) in the cell-attached and $0.75 \pm 0.08$ ($n = 17$) in the inside-out configuration.

## pH and $Ca^{2+}$ Dependence

The energy state of a cell may influence the intracellular pH. Since the activity of the ATP-inhibited $K^+$ channel is dependent on the energy state of the Retzius neuron, we investigated if changes in intracellular pH also influence channel activity.

The pH dependence of $P_o$ of the ATP-inhibited $K^+$ channel was investigated by altering the pH in the range of 6.1 to 9.0 at the cytoplasmic face of inside-out patches. The $P_o$ of the ATP-inhibited $K^+$ channel decreases by more than 90% when the pH at the cytoplasmic face of the membrane is reduced from physiological (~7.5) to acidic (6.1) pH values (Fig. 6).

The single channel parameters of the ATP-inhibited $K^+$ channel are $Ca^{2+}$ independent (*not shown*).

## Pharmacology

The sensitivity of the ATP-inhibited $K^+$ channel to the $K^+$ channel blockers glibenclamide, tolbutamide, TEA, $Ba^{2+}$ and $Cs^+$ was investigated by varying their concentration at the cytoplasmic face of inside-out patches.

Glibenclamide (10 nM) (Fig. 7) and 10 $\mu$M tolbutamide (Fig. 8) completely block the ATP-inhibited $K^+$ channel. The blocking effect of the sulfonylureas is irreversible and can be observed after 5 to 7 min of incubation. The upper recording in Fig. 8 shows an inside-out patch with one ATP-inhibited $K^+$ channel and one 30 pS channel in the absence of tolbutamide. Seven minutes after adding 10 $\mu$M tol-

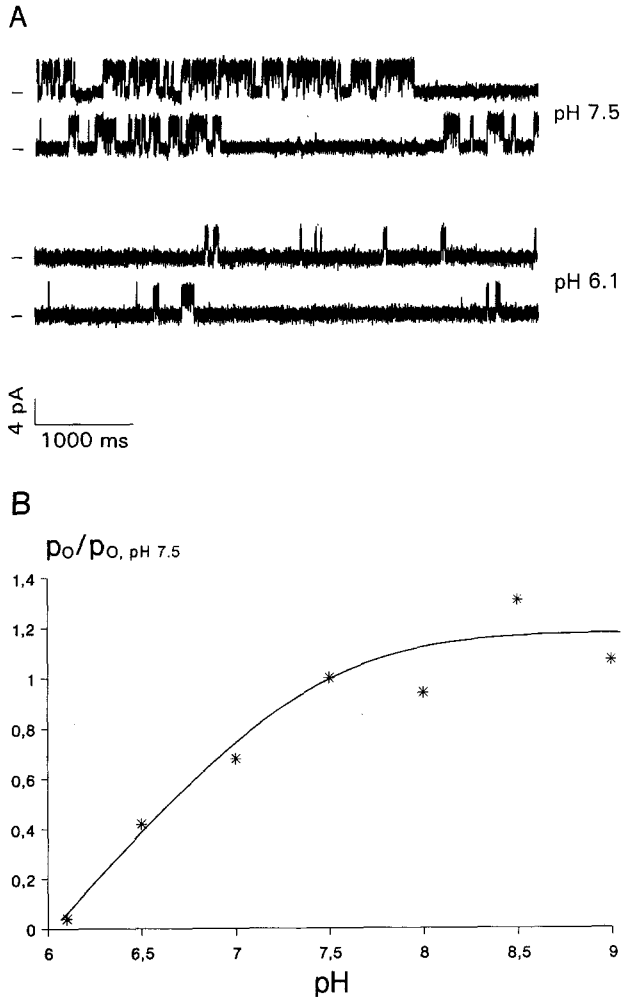


**Fig. 6.** pH dependence of the ATP-inhibited $K^+$ channel at the cytoplasmic face of inside-out patches. Recordings at pH 6.1 and 7.5 (*A*) and $P_o/P_{o,\ 7.5}$/pH plot (*B*) [−40 mV holding potential; symmetrical 120 mM $K^+$ solution, bath pH 6.1 and pH 7.5, pipette pH 7.5; $n = 4$]. In *B* the $P_o$ values are standardized to the $P_o$ values at pH 7.5 for a better comparison of the experiments. Altering the pH at the cytoplasmic face of the membrane from 7.5 to 6.1 reduced $P_o$ by more than 90%. An increase of the pH value from 7.5 to 9.0 enhanced $P_o$ only slightly.


**Fig. 7.** The effect of glibenclamide on the ATP-inhibited $K^+$ channel. Recordings in the inside-out configuration in symmetrical 120 mM $K^+$ solution at a holding potential of −60 mV. The upper recording shows an ATP-inhibited $K^+$ channel in the absence of glibenclamide (control). Glibenclamide (10 nM) (lower recording) blocks the channel irreversibly 7 min after application.


**Fig. 8.** The effect of tolbutamide on the ATP-inhibited $K^+$ channel and on a 30 pS channel. Recordings in the inside-out configuration in symmetrical 120 mM $K^+$ solution at a holding potential of −60 mV. The upper recording shows one 30 pS and one ATP-inhibited $K^+$ channel in the absence of tolbutamide (control). The bar indicates the closed state, the arrows (beginning at the closed state) the open state of the 30 pS channel, of the ATP-inhibited $K^+$ channel and of both channels simultaneously. Tolbutamide (10 μM) irreversibly blocks the ATP-inhibited $K^+$ channel 6 min after application, whereas the 30 pS channel remains unaffected (lower recording).

butamide to the cytoplasmic face of the membrane the ATP-inhibited $K^+$ channel is completely blocked, whereas the 30 pS channel is unaffected (lower recording in Fig. 8; symmetrical 120 mM $K^+$ solution, −60 mV holding potential).

TEA reversibly reduces the single channel amplitude of the ATP-inhibited $K^+$ channel. The relation between TEA concentration in the bathing solution and current amplitude standardized to the current amplitude in the absence of TEA ($I_{TEA}/I_{control}$) is plotted in Fig. 9. TEA (0.8 mM) is required for half-maximal inhibition of the ATP-inhibited $K^+$ channel at the cytoplasmic face of the membrane (inside-out configuration, symmetrical 120 mM $K^+$ solution, −40 mV holding potential; Fig. 9).

The ATP-inhibited $K^+$ channel is completely blocked by 10 mM $Ba^{2+}$ (inside-out configuration, symmetrical 120 mM $K^+$ solution, +40 mV holding potential, $n = 4$; Fig. 10). $Cs^+$ (50 mM) blocks less than 25% of the single channel amplitude.

## $Ca^{2+}$-Dependent $K^+$ Channel

The properties of a $Ca^{2+}$-dependent $K^+$ channel are shown in Fig. 11 (inside-out configuration, −40 mV holding potential, symmetrical 120 mM $K^+$ solution): (*A*) shows the recordings of channel fluctuations and (*B*) the amplitude histogram. (*C*) and (*D*) show the lifetime distributions of the closed and open states.

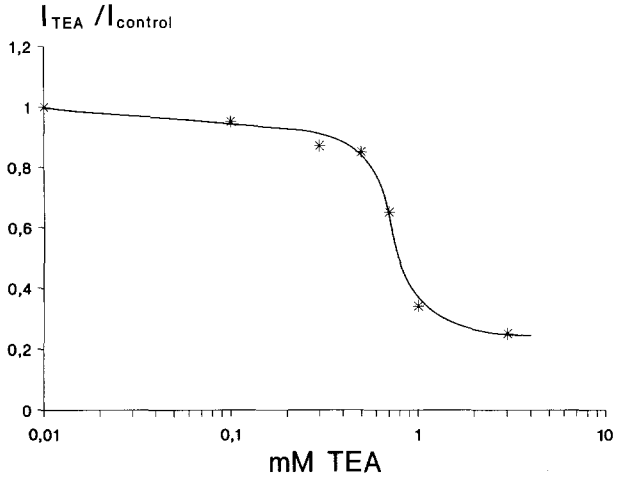


**Fig. 9.** TEA sensitivity of the ATP-inhibited $K^+$ channel at the cytoplasmic face of inside-out patches. Relation between TEA concentration in the bathing solution and current amplitude $I$ in the presence of TEA ($I_{TEA}$) standardized to $I$ in the absence of TEA ($I_{control}$) (symmetrical 120 mM $K^+$ solution, −40 mV holding potential). TEA reduces the current amplitude with a $K_i$ value of 0.8 mM.

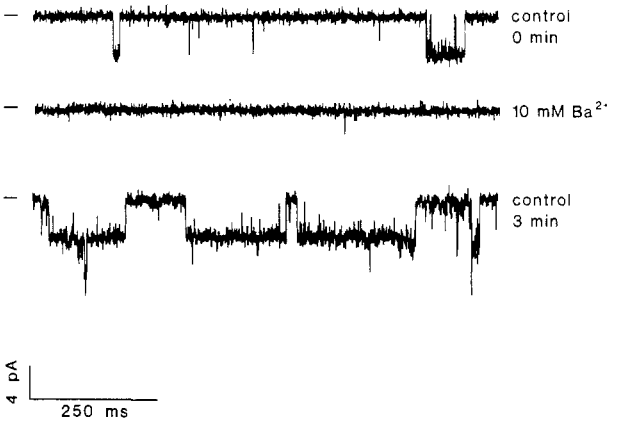


**Fig. 10.** $Ba^{2+}$ sensitivity of the ATP-inhibited $K^+$ channel. Recordings in the inside-out configuration in symmetrical 120 mM $K^+$ solution at a holding potential of +40 mV. The ATP-inhibited $K^+$ channel is completely blocked by 10 mM $Ba^{2+}$.

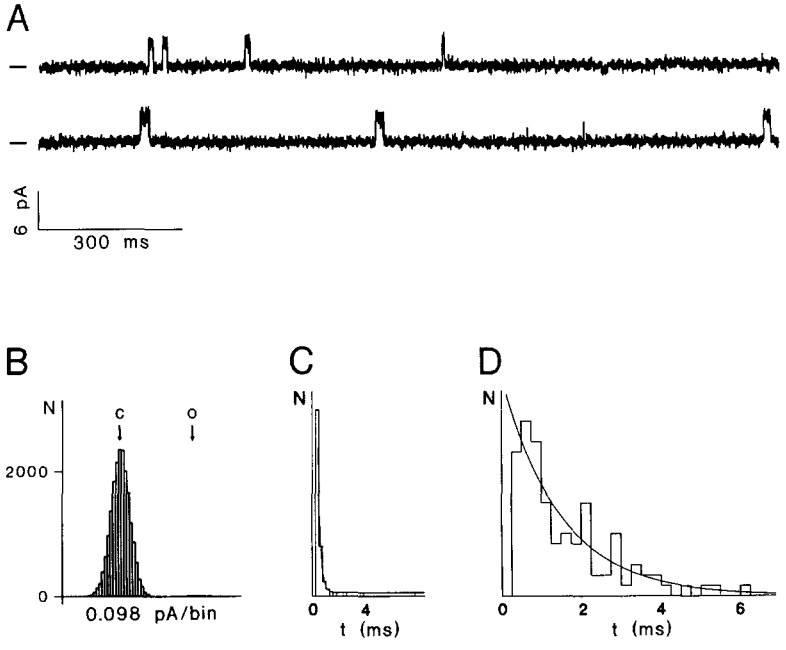


**Fig. 11.** Properties of a $Ca^{2+}$-dependent $K^+$ channel: Recordings (*A*), amplitude histogram (*B*), and lifetime distribution of the closed (*C*) and open (*D*) states [inside-out configuration, symmetrical 120 mM $K^+$ solution, −40 mV holding potential]. The open state lifetimes are single exponentially distributed with $t_o$ = 1.5 msec and the closed state lifetimes are double exponentially distributed with $t_{c1}$ = 0.2 msec and $t_{c2}$ = 305.4 msec.

The open state lifetimes are single exponentially distributed with a mean lifetime of $t_o$ = 1.5 msec. The closed state lifetimes are double exponentially distributed with $t_{c1}$ = 0.2 msec and $t_{c2}$ = 305.4 msec, thus indicating a bursting behavior of the channel. The $P_o$ was less than 0.01.

## $Ca^{2+}$ Dependence

The $Ca^{2+}$ dependence of the channel was analyzed by changing the free $Ca^{2+}$ concentration at the cytoplasmic face of excised inside-out patches. Figure 12 shows the dependence of the $Ca^{2+}$-dependent $K^+$

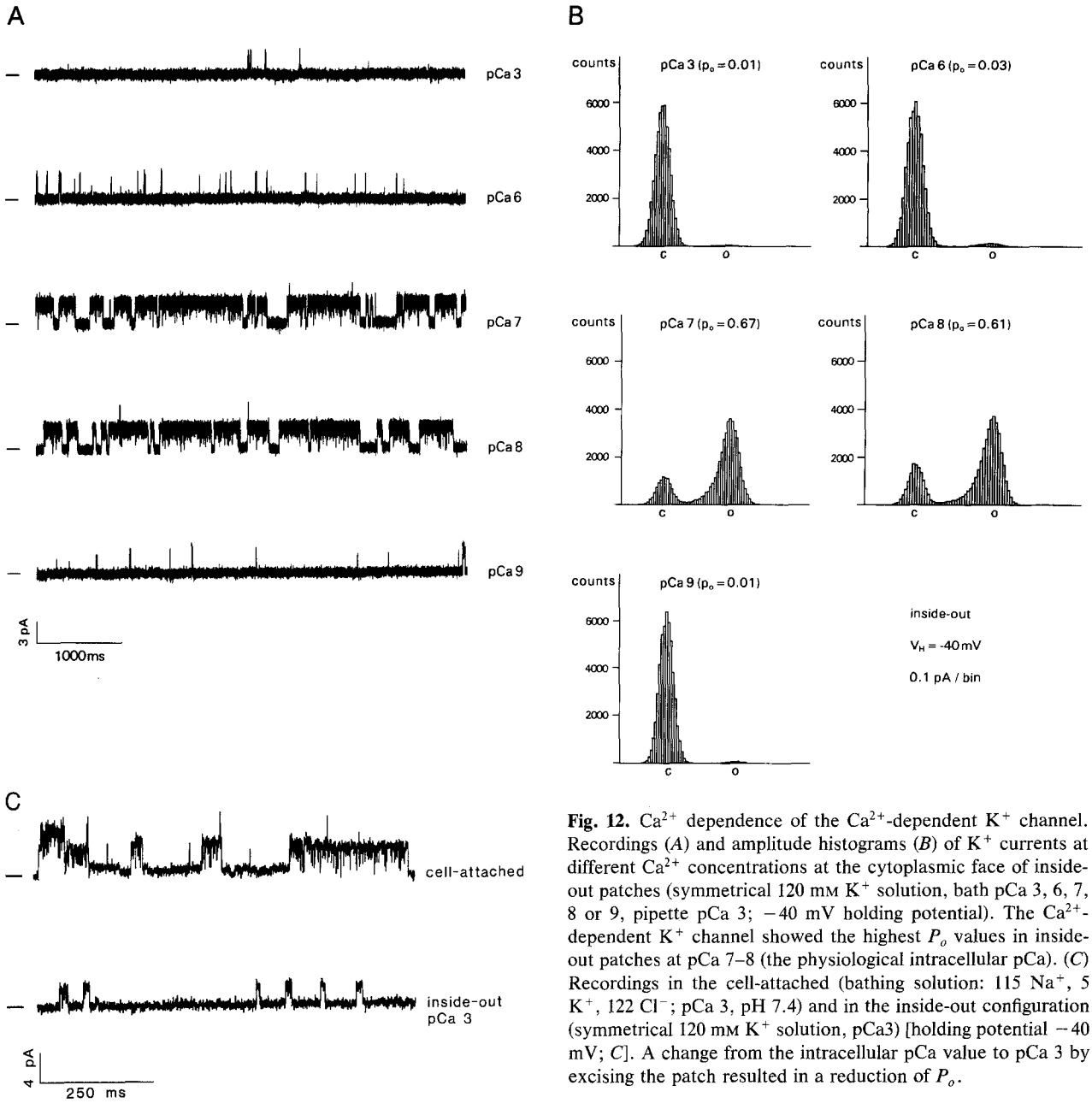


**Fig. 12.** $Ca^{2+}$ dependence of the $Ca^{2+}$-dependent $K^+$ channel. Recordings (*A*) and amplitude histograms (*B*) of $K^+$ currents at different $Ca^{2+}$ concentrations at the cytoplasmic face of inside-out patches (symmetrical 120 mM $K^+$ solution, bath pCa 3, 6, 7, 8 or 9, pipette pCa 3; −40 mV holding potential). The $Ca^{2+}$-dependent $K^+$ channel showed the highest $P_o$ values in inside-out patches at pCa 7–8 (the physiological intracellular pCa). (*C*) Recordings in the cell-attached (bathing solution: 115 $Na^+$, 5 $K^+$, 122 $Cl^-$; pCa 3, pH 7.4) and in the inside-out configuration (symmetrical 120 mM $K^+$ solution, pCa3) [holding potential −40 mV; *C*]. A change from the intracellular pCa value to pCa 3 by excising the patch resulted in a reduction of $P_o$.

channel on the $Ca^{2+}$ concentration of the bathing solution (inside-out configuration, −40 mV holding potential, symmetrical 120 mM $K^+$ solution of pCa 3, 6, 7, 8, 9 [bath] and pCa 3 [pipette]). The recordings in (*A*) and the appropriate amplitude histograms in (*B*) reveal a bell-shaped $Ca^{2+}$ dependence of this type of $K^+$ channel: it has a maximum activity at pCa 7–8 and is less active at lower and higher free $Ca^{2+}$ concentrations ($P_o$ = 0.03 at pCa 6, $P_o$ = 0.67 at pCa 7, $P_o$ = 0.61 at pCa 8, $P_o$ = 0.01 at pCa 9). The enhancement of $P_o$ in the pCa range of 7–8 is due as much to an increase in the opening frequency as to an increase in the effective duration of channel openings. $Ca^{2+}$ does not affect the current amplitude of the $Ca^{2+}$-dependent $K^+$ channel.

For further evidence we compared the activity of the $Ca^{2+}$-dependent $K^+$ channel in the cell-attached configuration and in the inside-out configuration at pCa 3 (Fig. 12*C*). The recordings in Fig. 12*C* indicate that the activity of this channel is higher in the cell-attached configuration than in the inside-out configuration at pCa 3 (−40 mV holding potential; bathing solution: 115 $Na^+$, 5 $K^+$, 122 $Cl^-$; pCa 3, pH 7.4 (cell-attached), 120 mM $K^+$ solution (inside-out)).

The investigation of the $Ca^{2+}$-dependent $K^+$

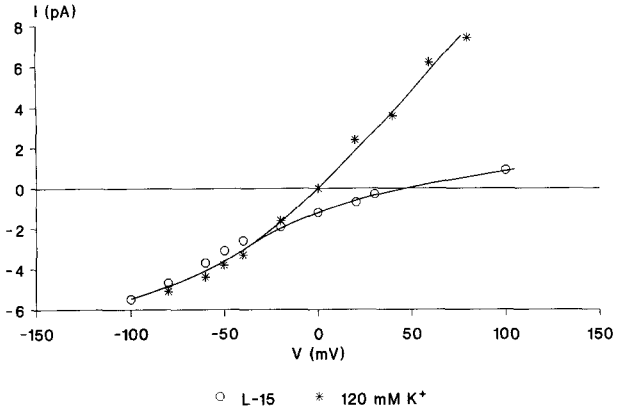


**Fig. 13.** Ion selectivity and rectification of the $Ca^{2+}$-dependent $K^+$ channel. The *I/V* plots in the inside-out configuration with 120 mM $K^+$ solution ($n = 7$) and with L-15 as bathing solution ($n = 7$) indicate that the $Ca^{2+}$-dependent $K^+$ channel is selective for $K^+$ over $Na^+$: The *I/V* plot with L-15 as bathing solution bends at positive voltages and reveals a reversal potential of about +50 mV. According to the Goldman-Hodgkin-Katz-equation a permeability ratio ($P_K/P_{Na}$) of 13 can be calculated.

The *I/V* plot in the inside-out configuration in symmetrical 120 mM $K^+$ solution demonstrates the rectifying characteristics of this channel type at negative voltages.

channel was difficult because of the high $P_o$ values of the ATP-inhibited $K^+$ channel. Since both types of $K^+$ channels differ largely in their $P_o$ values and kinetics at pCa 3 in the inside-out configuration (Figs. 1 and 11) we performed most of the experiments in solutions of pCa 3 to be able to distinguish between the two channel types.

## Ion Selectivity, Rectification and Voltage Dependence

Ion substitution experiments at the cytoplasmic face of inside-out patches reveal that the $Ca^{2+}$-dependent $K^+$ channel is selective for $K^+$ over $Na^+$, $NH_4^+$, and $Rb^+$. Figure 13 shows an *I/V* plot of the channel with 120 mM $K^+$ solution and L-15 as bathing solution. The *I/V* plot with L-15 as bathing solution shows rectification at positive potentials. The reversal potential of about +50 mV reveals a permeability coefficient ($P_K/P_{Na}$) of 13.

Because of the poor signal to noise ratio it was not possible to obtain current values close to the reversal potentials of the ATP-inhibited and the $Ca^{2+}$-dependent $K^+$ channel. Thus, the different reversal potentials are not reliable enough to distinguish between the two types of $K^+$ channel.

The *I/V* plot in the inside-out configuration in symmetrical 120 mM $K^+$ solution (Fig. 13) indicates the rectifying characteristics of the $Ca^{2+}$-dependent $K^+$ channel. This type of $K^+$ channel

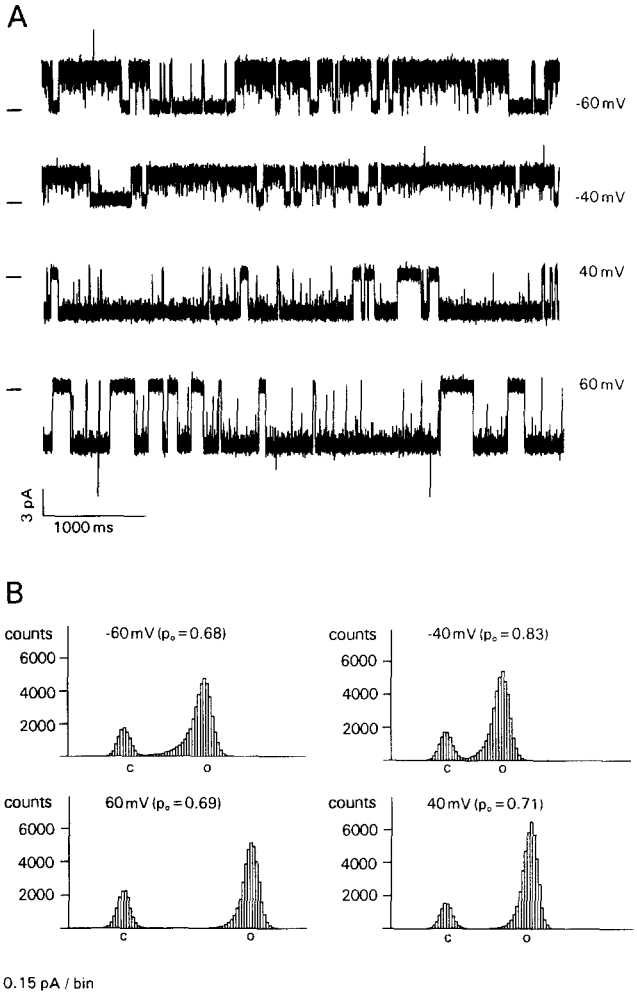


**Fig. 14.** Voltage dependence of the $Ca^{2+}$-dependent $K^+$ channel with pCa 7 at the cytoplasmic face of an inside-out patch; recordings (*A*) and amplitude histograms (*B*) [symmetrical 120 mM $K^+$ solution, pipette pCa 3]. The recordings and the amplitude histograms show that the channel activity is not voltage dependent in the measured *V* range of +60 to −60 mV.

rectifies—similar to the ATP-inhibited $K^+$ channel—at negative voltages. Because of the instability of the seals at positive voltages and the difficulties in achieving data for this channel type, there are no data available at voltages above +80 mV.

The voltage dependence of $P_o$ of the $Ca^{2+}$-dependent $K^+$ channel was analyzed in the inside-out configuration. The excised patches were superfused with symmetrical 120 mM $K^+$ solution of either pCa 7 (Fig. 14) or pCa 3 (Fig. 15). Figures 14*A* and 15*A* show the recordings of the channel at different voltages and Fig. 14*B* the amplitude histograms belonging to 14*A*. The mean $P_o$ values of the channel with pCa 3 at the cytoplasmic face of the membrane are plotted *vs.* voltage in Fig. 15*B* ($n = 10$).

At pCa 7 the $P_o$ of the $Ca^{2+}$-dependent $K^+$ chan-

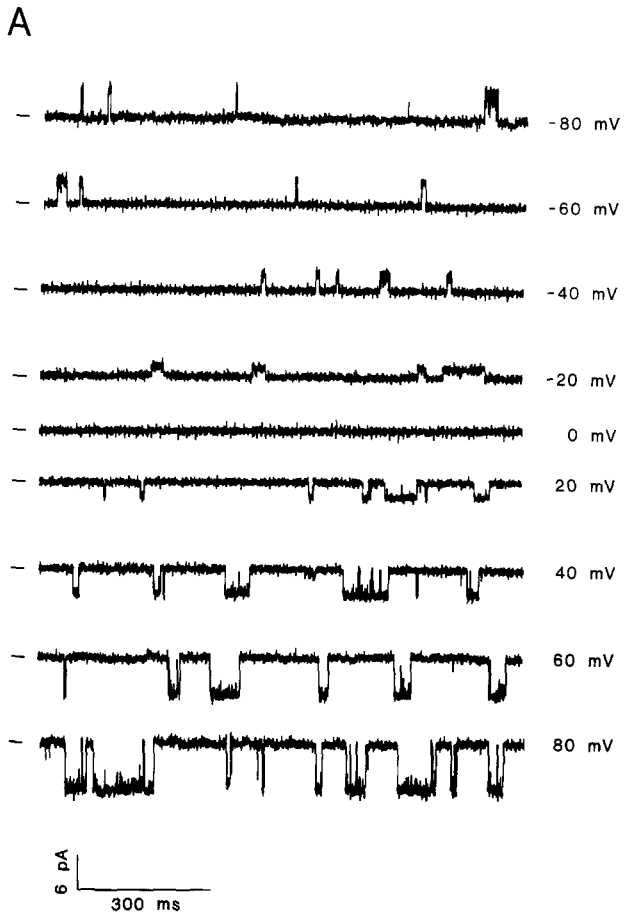


**Fig. 15.** Voltage dependence of the open state probabilities ($P_o$) of the $Ca^{2+}$-dependent $K^+$ channel. Recordings at different voltages (*A*) and $P_o/V$ plot (*B*) [inside-out configuration, symmetrical 120 mM $K^+$ solution]. The $P_o/V$ plot in (*B*) ($n = 10$) shows that $P_o$ of the $K^+$ channel increases at positive voltages above +70 mV.

nel is voltage independent at the physiological relevant $V$ range (−60 to +60 mV). At pCa 3 $P_o$ increases at positive voltages above +70 mV.

A comparison of the recordings in Fig. 14*A* (pCa 7) and Fig. 15*A* (pCa 3) reveal that the block

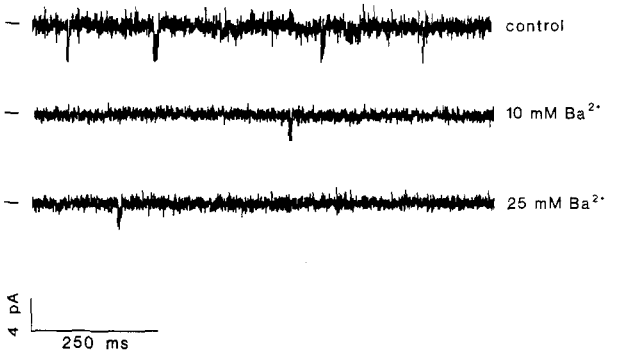


**Fig. 16.** $Ba^{2+}$ sensitivity of the $Ca^{2+}$-dependent $K^+$ channel. Recordings in the inside-out configuration in symmetrical 120 mM $K^+$ solution at a holding potential of +40 mV. $Ba^{2+}$ (10 mM) reduces the current amplitude by 25 ± 5% and 25 mM $Ba^{2+}$ by 36 ± 7% of the control amplitude ($n = 4$).

of the channel at high internal $Ca^{2+}$ concentrations is voltage independent in the measured $V$ range.

### Pharmacology

The sensitivity of the $Ca^{2+}$-dependent $K^+$ channel to the $K^+$ channel blockers $Ba^{2+}$ and $Cs^+$ was investigated by varying their concentration at the cytoplasmic face of inside-out patches.

$Ba^{2+}$ (10 mM) reduces the single channel amplitude (Fig. 16) by 25 ± 5% and 25 mM reduces it by 36 ± 7% (inside-out configuration, symmetrical 120 mM $K^+$ solution, +40 mV holding potential, $n = 4$). The channel is less sensitive to $Cs^+$: 50 mM $Cs^+$ blocks less than 25% of the single channel amplitude. The $Ba^{2+}$ and $Cs^+$ sensitivity of the channel is voltage independent under our experimental conditions.

## Discussion

In the present study we have characterized two types of $K^+$ channels in the soma membrane of cultured leech Retzius neurons. These two types of $K^+$ channels are identical in their conductances of about 110 pS and in their outward rectifying characteristics. They can be discriminated by their $P_o$ values, their ATP and $Ca^{2+}$ dependence and their $Ba^{2+}$ sensitivity: One channel type is ATP and $Ba^{2+}$ sensitive but $Ca^{2+}$ independent under our experimental conditions (ATP-inhibited $K^+$ channel). The other channel type is $Ca^{2+}$ dependent, but less $Ba^{2+}$ sensitive ($Ca^{2+}$-dependent $K^+$ channel).

### ATP-Inhibited $K^+$ Channel

The ATP-inhibited $K^+$ channel is inhibited by intracellular ATP. Our experiments with inside-out

patches reveal that 100 $\mu$M ATP is needed for half-maximal inhibition. ATP (2 mM) at the cytoplasmic face of the Retzius cell membrane reduces the channel activity to the cell-attached activity (Fig. 2). This finding corresponds to an intracellular ATP concentration of about 8 mM in brain cells (Amoroso et al., 1990).

According to the classification of Ashcroft and Ashcroft (1990) the ATP-inhibited $K^+$ channel in the soma membrane of Retzius neurons belongs to type 1 K-ATP channels: Type 1 K-ATP channels are inhibited by micromolar concentrations of ATP applied to the intracellular membrane surface, and their channel activity is relatively insensitive to $Ca^{2+}$ and voltage. Type 1 K-ATP channels have already been described in cardiac muscle (Noma, 1983), skeletal muscle (Spruce, Standen & Stanfield, 1985), smooth muscle (Standen et al., 1989), pancreatic $\beta$-cells (Cook & Hales, 1984), and in vertebrate axons (Jonas et al., 1991), but not yet in the soma membrane of neurons.

We show that the ATP-inhibited $K^+$ channel in neurons is pH-dependent: A decrease of the pH at the cytoplasmic face of inside-out patches leads to a reduction of $P_o$. A similar pH dependence has already been described for the ATP-dependent $K^+$ channel in pancreatic $\beta$-cells (Misler, Gillis & Tabcharani, 1989), kidney cells (Ohno-Shosaku et al., 1990; Wang, Schwab & Giebisch, 1990), and ventricular myocytes (Cuevas et al., 1991).

## $Ca^{2+}$-Dependent $K^+$ Channel

The $Ca^{2+}$-dependent $K^+$ channel in the soma membrane of leech Retzius neurons belongs to the group of $Ca^{2+}$-dependent $K^+$ channels of intermediate conductance (Kolb, 1990). Macroscopically it contributes to $I_c$ ($Ca^{2+}$-activated $K^+$ current). The macroscopic current $I_c$ has already been described in leech Retzius neurons by Stewart, Nicholls and Adams (1989) and Garcia et al. (1990). On the single-channel level $Ca^{2+}$-activated $K^+$ channels were analyzed in growth cones of Retzius neurons and in the soma membrane of AP (anterior pagoda) neurons of the leech *H. medicinalis* (Pellegrini, Simoni & Pellegrino, 1989) and in ALG (anterior lateral giant) neurons of the leech *Haementeria ghilanii* (Yang et al., 1987).

The $Ca^{2+}$-dependent $K^+$ channel in the soma membrane of Retzius neurons shows a bell-shaped $Ca^{2+}$ dependence of $P_o$ with a maximum at pCa 7–8. Thus, this channel type is at maximum activity at the physiological intracellular pCa value of Retzius neurons (Deitmer & Schlue, 1983) and is blocked by intracellular $Ca^{2+}$ if the intracellular $Ca^{2+}$ concentration is raised. $Ca^{2+}$ blockade of $Ca^{2+}$-activated $K^+$ channels at high intracellular $Ca^{2+}$ concentrations has already been described in various tissues (Marty, 1981; Vergara & Latorre, 1983; Findlay, Dunne & Petersen, 1985; Benham et al., 1986; Bregestovski, Redkozubov & Alexeev, 1986; Latorre et al., 1989; Armstrong & Palti, 1991; Chen & Wong, 1991; Mukai, Kyogoku & Kuno, 1992).

We conclude that the *$Ca^{2+}$-dependent $K^+$ channel* in the soma membrane of leech Retzius neurons may play a role in generating the resting membrane potential because it shows maximum activity at the intracellular pCa value (Deitmer & Schlue, 1983).

*The ATP-inhibited $K^+$ channel* may play a role in maintaining the membrane potential constant—independently from the energy state of the cell. A low ATP level induces an opening of ATP-inhibited $K^+$ channels and thus a $K^+$ outward current. This outward current may compensate the depolarization induced by the blockade of ATP-dependent pumps (e.g., $Na^+/K^+$-ATPase) so that the membrane potential remains constant.

The ATP-inhibited $K^+$ channel may also prevent the Retzius neurons from an excessive $Ca^{2+}$ load, which leads to cell death (Siesjö, 1988): Retzius neurons possess voltage-dependent $Ca^{2+}$ channels (Bookman & Liu, 1990) which could be activated by the depolarization induced by the blockade of ATP-dependent pumps.

This study was supported by the Deutsche Forschungsgemeinschaft (W.-R. Schlue) and by a fellowship of the Konrad-Adenauer-Stiftung (G. Frey). We thank Dr. Draeger (Hoechst AG) for the gift of glibenclamide. The data are part of a future Ph.D. thesis of G. Frey.

## References

Ammann, D., Bührer, T., Schefer, U., Müller, M., Simon, W. 1987. Intracellular neutral carrier-based $Ca^{2+}$ microelectrode with subnanomolar detection limit. *Pfluegers Arch.* **409:**223–228

Amoroso, S., Schmid-Antomarchi, H., Fosset, M. Lazdunski, M. 1990. Glucose, sulfonylureas, and neurotransmitter release: role of ATP-sensitive $K^+$ channels. *Science* **247:** 852–854

Armstrong, C.M., Palti, Y. 1991. Potassium channel block by internal calcium and strontium. *J. Gen. Physiol.* **97:** 627–638

Ashcroft, F.M. 1988. Adenosine 5'-triphosphate-sensitive potassium channels. *Annu. Rev. Neurosci.* **11:**97–118

Ashcroft, S.J.H., Ashcroft, F.M. 1990. Properties and functions of ATP-sensitive K-channels. *Cell. Signal.* **2:** 197–214

Benham, C.D., Bolton, T.B., Lang, R.J., Takewaki, T. 1986. Calcium-activated potassium channels in single smooth muscle cells of rabbit jejunum and guinea-pig mesenteric artery. *J. Physiol.* **371:**5–67

Bookman, R.J., Dagan, D. 1987. Single $K^+$ channel activity recorded from leech neurons in culture. *J. Physiol.* **390:**76P

Bookman, R.J., Liu, Y. 1990. Analysis of calcium channel properties in cultured leech Retzius cells by internal perfusion, volt-

age-clamp and single-channel recording. *J. Exp. Biol.* **149:**223–237

Bregestovski, P., Redkozubov, A., Alexeev, A. 1986. Elevation of intracellular calcium reduces voltage-dependent potassium conductance in human T cells. *Nature* **319:**776–778

Chen, Q.X., Wong, R.K.S. 1991. Intracellular $Ca^{2+}$ suppressed a transient potassium current in hippocampal neurons. *J. Neurosci.* **11(2):**337–343

Cook, D.L., Hales, N. 1984. Intracellular ATP directly blocks $K^+$ channels in pancreatic B-cells. *Nature* **311:**271–273

Cuevas, J., Bassett, A.L., Cameron, J.S., Furukawa, T., Myerburg, R.J., Kimura, S. 1991. Effect of $H^+$ on ATP-regulated $K^+$ channels in feline ventricular myocytes. *Am. J. Physiol.* **261:**H755–761

Deitmer, J.W., Schlue, W.R. 1983. Intracellular $Na^+$ and $Ca^{2+}$ in leech Retzius neurones during inhibition of the $Na^+$-$K^+$ pump. *Pfluegers Arch.* **397:**195–201

Dietzel, I.D., Drapeau, P., Nicholls, J.G. 1986. Voltage dependence of 5-hydroxytryptamine release at a synapse between identified leech neurones in culture. *J. Physiol.* **372:**191–205

Findlay, I., Dunne, M.J., Petersen, O.H. 1985. High conductance $K^+$ channel in pancreatic islet cells can be activated and inactivated by internal calcium. *J. Membrane Biol.* **83:**169–175

Garcia, U., Grumbacher-Reinert, S., Bookman, R., Reuter, H. 1990. Distribution of $Na^+$ and $K^+$ currents in soma, axons and growth cones of leech Retzius neurones in culture. *J. Exp. Biol.* **150:**1–17

Hamill, O.P., Marty, A., Neher, E., Sakmann, B., Sigworth, F.J. 1981. Improved patch-clamp techniques for high-resolution current recording from cells and cell-free membrane patches. *Pfluegers Arch.* **391:**85–100

Jonas, P., Koh, D.S., Kampe, K., Hermsteiner, M., Vogel, W. 1991. ATP-sensitive and Ca-activated K channels in vertebrate axons: novel links between metabolism and excitability. *Pfluegers Arch.* **418:**68–73

Kolb, H.A. 1990. Potassium channels in excitable and non-excitable cells. *Rev. Physiol. Biochem. Pharmacol.* **115:**51–91

Latorre, R., Miller, C. 1983. Conduction and selectivity in potassium channels. *J. Membrane Biol.* **71:**11–30

Latorre, R., Oberhauser, A., Labarca, P., Alvarez, O. 1989. Varieties of calcium-activated potassium channels. *Annu. Rev. Physiol.* **51:**385–399

Lent, C.M. 1973. Retzius cells: neuroeffectors controlling mucus release by the leech. *Science* **179:**693–696

Marty, A. 1981. Ca-dependent potassium channel with large unitary conductance in chromaffin cell membranes. *Nature* **291:**497–500

Mason, A., Kristan, W.B., Jr. 1982. Neuronal excitation, inhibition and modulation of leech longitudinal muscle. *J. Comp. Physiol.* **146:**527–536

Misler, S., Gillis, K., Tabcharani, J. 1989. Modulation of gating of a metabolically regulated, ATP-dependent $K^+$ channel by intracellular pH in B cells of the pancreatic islet. *J. Membrane Biol.* **109:**135–143

Mukai, M., Kyogoku, I., Kuno, M. 1992. Calcium-dependent inactivation of inwardly rectifying $K^+$ channel in a tumor mast cell line. *Am. J. Physiol.* **262:**C84–C90

Noma, A. 1983. ATP-regulated $K^+$ channels in cardiac muscle. *Nature* **305:**147–148

Ohno-Shosaku, T., Kubota, T., Yamaguchi, J., Fujimoto, M. 1990. Regulation of inwardly rectifying $K^+$ channels by intracellular pH in opossum kidney cells. *Pfluegers Arch.* **416:**138–143

Pellegrini, M., Simoni, A., Pellegrino, M. 1989. Two types of $K^+$ channels in excised patches of somatic membrane of the leech AP neuron. *Brain Res.* **483:**294–300

Rudy, B. 1988. Diversity and ubiquity of K channels. *Neurosci.* **25:**729–749

Schlue, W.R., Deitmer, J.W. 1980. Extracellular potassium in neuropile and nerve cell body region of the leech central nervous system. *J. Exp. Biol.* **87:**23–43

Schlue, W.R., Deitmer, J.W. 1988. Ionic mechanisms of intracellular pH regulation in the nervous system. *In:* Proton Passage across Cell Membranes. Ciba Foundation Symposium 139; pp. 47–69. Wiley, Chichester

Schwarz, W., Passow, H. 1983. $Ca^{2+}$-activated $K^+$ channels in erythrocytes and excitable cells. *Annu. Rev. Physiol.* **45:**359–374

Siesjö, B.K. 1988. Calcium, ischemia, and death in rat brain in vivo. *Ann. N.Y. Acad. Sci.* **522:**638–661

Spruce, A.E., Standen, N.B., Stanfield, P.R. 1985. Voltage-dependent ATP-sensitive potassium channels of skeletal muscle membrane. *Nature* **316:**736–738

Standen, N.B., Quayle, J.M., Davies, N.W., Brayden, J.E., Huang, Y., Nelson, M.T. 1989. Hyperpolarizing vasodilators activate ATP-sensitive $K^+$ channels in arterial smooth muscle. *Science* **245:**177–180

Stewart, R.R., Nicholls, J.G., Adams, W.B. 1989. $Na^+$, $K^+$ and $Ca^{2+}$ currents in identified leech neurones in culture. *J. Exp. Biol.* **141:**1–20

Vergara, C., Latorre, R. 1983. Kinetics of $Ca^{2+}$-activated $K^+$ channels from rabbit muscle incorporated into planar bilayers. Evidence for a $Ca^{2+}$ and $Ba^{2+}$ blockade. *J. Gen. Physiol.* **82:**543–568

Wang, W.H., Schwab, A., Giebisch, G. 1990. Regulation of small-conductance $K^+$ channel in apical membrane of rat cortical collecting tubule. *Am. J. Physiol.* **259:**F494–502

Willard, A.L. 1981. Effects of serotonin on the generation of the motor program for swimming by the medicinal leech. *J. Neurosci.* **1:**936–944

Yang, J., Johansen, J., Koehm, S., Kleinhaus, A.L. 1987. In situ patch-clamp recording of calcium-activated potassium channels from identified leech neuron. *Brain Res.* **419:**324–328